Towards an efficient inverse characterization of the viscoelastic properties of anisotropic media based on the Ultrasonic Polar Scan

A. Martens[1 a)], M. Kersemans[2], J. Daemen[1], E. Verboven[2], W. Van Paepegem[2], J. Degrieck[2], S. Delrue[1], K. Van Den Abeele[1]

[1]*Wave Propagation and Signal Processing (WPSP), Department of Physics, KU Leuven-Kulak, 8500 Kortrijk, Belgium*
[2]*Mechanics of Materials and Structures (MMS), Ghent University, Technologiepark-Zwijnaarde 903, 9052 Zwijnaarde, Belgium*

[a)]Corresponding author: arvid.martens@kuleuven.be

Abstract. Composite materials (e.g. carbon fiber reinforced plastics (CFRP)) are increasingly used for critical components in several industrial sectors (e.g. aerospace, automotive,…). Their anisotropic nature makes it difficult to accurately determine material properties or to assess internal damages. To resolve these challenges, the Ultrasonic Polar Scan (UPS) technique has been introduced. In a UPS experiment, a fixed material spot is insonified at a multitude of incidence angles $\Psi(\theta,\varphi)$ for which the transmission amplitude as well as the associated arrival time (time-of-flight) are measured. Mapping these quantities on a polar diagram represents a fingerprint of the local viscoelasticity of the investigated material. In the present study, we propose a novel two-stage inversion scheme which is able to infer both the elastic and the viscous properties. In the first step, we solve the inverse problem of determining the elastic constants from time-of-flight UPS recordings. The second stage handles a similar inverse problem, but now operates on the amplitude landscape of a UPS experiment for determining the viscous part of the viscoelastic tensor. This two-stage procedure thus yield the viscoelastic tensor of the insonified material spot. The developed characterization scheme has been employed on both virtual (numerical) UPS recordings, to test the effectiveness of the method, and experimental UPS recordings of unidirectional C/E plates.

INTRODUCTION

The ongoing pursuit of industry towards constructing stronger and lighter critical components of structures e.g. aircraft, pushes the development and innovation towards new and advanced materials. One class of new materials involves composite materials, such as sandwich structures (e.g. honeycomb) and fiber reinforced plastics. Of particular interest are the Carbon Fiber Reinforced Plastics (CFRP), which exploit the benefits of the high stiffness of carbon fibers and the low weight of polymer matrix, resulting in a material with high stiffness-to-weight ratio. These structural benefits however, come at a price as these composites comprise an intricate internal structure, characterized by a high degree of anisotropy of the viscoelastic material parameters. This anisotropic dependency obviously complicates the mechanical characterization of these materials. Indeed, whereas isotropic materials (e.g. aluminum, steel) are determined by solely two independent complex parameters (Young's modulus and shear modulus), one easily requires between five and nine complex valued constants (real and imaginary part denotes the elasticity and viscosity respectively) for commonly used CFRP materials. A major consequence of the difficult characterization process is that it is harder to design new composite materials, as full knowledge of the material parameters is needed to assure an optimal functionality of components constructed from this material.

In the past, several ultrasound based non-destructive testing techniques addressing the characterization and damage detection process have been introduced[1–4]. On the characterizing end of the problem, relative success was found in techniques making use of bulk wave approximations to infer information about the elastic properties of anisotropic

materials[3,5–9]. The power of these techniques relies on the intimate relation between the mechanical stiffness constants and the phase velocity (associated with the Time-of-Flight) of a transmitted ultrasonic pulse. Additionally, it has been proven that this characterization method can also be employed, with relative success, to retrieve information on the viscous properties of the material, by comparing amplitude levels of the measured signal with those of a theoretical estimate[1]. In spite of this, the current authors recently identified several limitations of the elastic determination techniques based on the principle of bulk wave propagation[10,11]:

- Bulk wave propagation is only valid when the wavelength of the waves is negligible compared to the thickness of the plate. In this regime, the investigated sample can be considered an 'infinite' medium and thus promotes bulk wave propagation. In reality, however, composite materials are mostly laminated structures containing a stacking of thin individual layers. Hence, a high frequency needs to be selected in order to remain in the bulk wave approximation. On the other hand, composite materials also exhibit a high amount of damping, e.g. due to viscosity and wave scattering at fiber bundles, which requires a sufficiently low frequency. In addition, the current authors[10] have proven that, even if a suitable frequency value has been determined for a region of incident angles, it is not valid to assume that the bulk wave approximation holds for all possible combinations of incidence angles.
- Most ultrasonic characterization techniques employ external borne ultrasound and a coupling medium (e.g. water), implying that the incident and scattered waves propagate in a different medium surrounding the sample and that the interaction with interfaces at either side of the plate have to be considered. The consequence of these interfaces is that a non-zero phase factor, resulting from the evanescent behavior of wave modes beyond their critical angle, has to be accounted for. For input signals containing an oscillatory term this phase factor shows up as a time delay. This phenomenon is generally neglected by the bulk wave based characterization methods as they assume propagation in unbounded media where no interfaces are present. A somewhat artificial modification to the bulk wave methods has been introduced by adding an ad-hoc time-delay, hence taking into account the effect of the interfaces[12]. However, upon decreasing the frequency or the thickness, interference effects of different wave modes and internal reflections will come into play in such a way that adding a time delay is not sufficient to invert for the elastic data, as the applied correction is only interface related and thus independent of the thickness.
- Most ultrasonic characterization approaches require a-priori knowledge about the direction of the material symmetry axes. This necessity relates to the fact that many of the applied inversion techniques are based on oblique angle (θ) ultrasonic scans at a few in-plane directions (φ = 0°, 90°, 45°)[1,2,4]. For isotropic materials (e.g. aluminum) this is not a problem as the wave propagation is independent of the direction in which it propagates. For materials with a lower symmetry class, e.g. composites, the wave response is dependent on the propagation direction. For this case, the correct selection of azimuthal angles (0°,45°,90°) is crucial in order to get a stable and correct inversion. Though, in reality, this selection is far from straightforward without a priori knowledge on the material symmetry of the investigated material.

A solution which resolves all of the above mentioned limitations is offered by the Ultrasonic Polar Scan (UPS). Although introduced around the same time (1980's) as the bulk wave based techniques and considered as a promising tool in the field of non-destructive testing[13–15], it took until recently to fully establish the technique as a pragmatic means of characterizing elastic material properties and internal damage phenomena[10,11,16–18]. The operating principle of the UPS is to insonify a specific material spot on a plate-like sample with an ultrasonic pulse directed at an incidence angle $\Psi(\theta,\varphi)$, where θ and φ correspond to spherical coordinate angles, and subsequently measuring the scattered wave characteristics (TOF, amplitude) in reflection or transmission. The angle of incidence is then changed until ideally the entire hemisphere (Figure 1a) above the material spot is scanned. Finally, a representation of the measured data is found by mapping the analyzed data in a polar coordinates figure where φ (in-plane orientation) corresponds to the angular direction and θ (vertical incident angle) to the radial direction. An example of a UPS experiment for a $[0°]_8$ C/E composite is shown in Figure 1b. The contours in such a UPS image are linked to the viscoelastic properties of the scanned material spot [10,16,18]. For instance, an isotropic material has perfectly circular features as the wave properties are independent of its in-plane propagation direction, while non-circular contours indicate that the material under investigation belongs to a lower symmetry class. This can be clearly seen in figure 1b, in which the stretched contours indicate the transversal isotropic character of the $[0]_8$ C/E.

In recent studies, we demonstrated the performance of an inversion routine to quantitatively determine the set of nine elastic constants of a general orthotropic material based on virtual (simulated) experiments of a Time-of-Flight Pulsed Ultrasonic Polar Scan (TOF P-UPS)[10]. The success of this inversion algorithm is based on the fact that elastic parameters are almost exclusively connected to the propagation speed of ultrasonic waves, and in a much lesser extent to viscous parameters. On the other hand, viscosity is the main contributor to the damping of an ultrasonic wave and

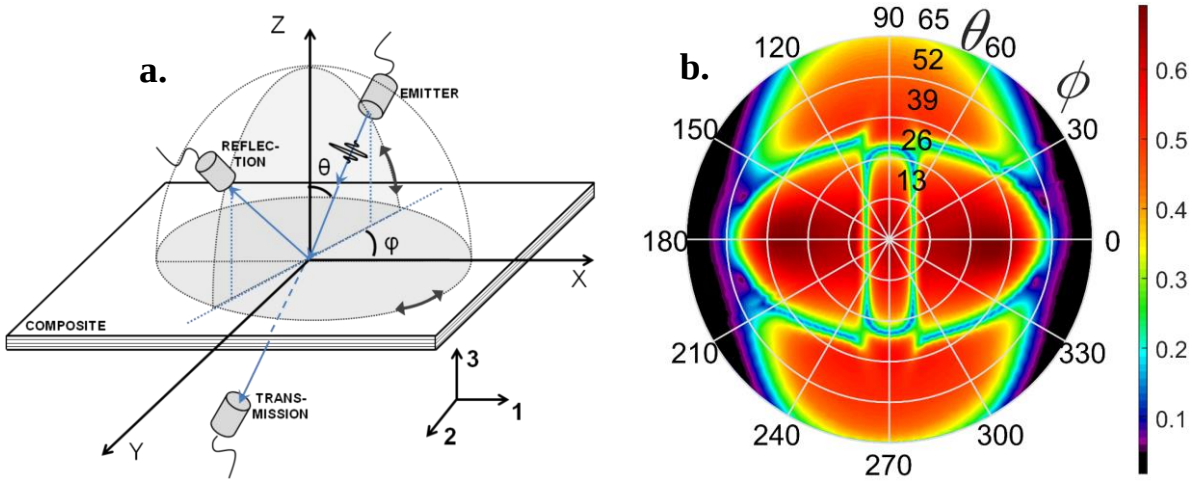

Figure 1: Scheme of the UPS operating principle (a). Note that the sound emitting/receiving transducer are located in a water tank to enhance ultrasound coupling into the material. Transmission amplitude P-UPS experiment (colorbar normalized to input amplitude) for a $[0°]_8$ C/E composite at frequency-thickness $f_c d$ = 5 MHz.mm (b). Remark that the non-circular characteristic contours indicate the anisotropic nature of the scanned $[0]_8$ C/E.

therefore mostly visible in the amplitude landscape of a P-UPS measurement. To account for both contributions, a two-stage approach for the determination of the complex viscoelastic tensor will be introduced in this paper. Stage one of the approach is a TOF P-UPS based inversion of the elasticity constants, whereas stage two introduces a similar inversion strategy, but now applied on the amplitude P-UPS data to infer the viscous parameters. The methodology will be first tested on artificial UPS data, which was generated by a forward numerical UPS model, in order to test the effectiveness and robustness. Finally, first experimental inversion results are shown for the determination of the elastic constants of a $[0°]_4$ C/E plate.

THEORETICAL BACKGROUND

Modeling the wave propagation in anisotropic media

A good starting point to model the propagation of a linear wave inside a generally anisotropic material is the Christoffel equation (eq. 1), which combines Hooke's law and Newton's second law with the general expression of a linear harmonic wave.

$$(C_{ijkl} k_j k_k - \rho\omega^2 \delta_{i,l}) U_l = 0 \tag{1}$$

Here, C_{ijkl} denotes the viscoelastic tensor components, k_i the components of the wave vector (3 cartesian components), ρ the density of the material, ω the angular frequency of the incident wave and U_i the components of the polarization vector. Einstein notation is assumed. The equation represents an eigenvalue problem and can be solved for one component of the wave vector (e.g. k_3) considering that the two other components are determined by Snell's law. After some algebra, a sixth order polynomial in the k_3 component is obtained (eq. 2).

$$\beta_6 k_3^6 + \beta_5 k_3^5 + \beta_4 k_3^4 + \beta_3 k_3^3 + \beta_2 k_3^2 + \beta_1 k_3^1 + \beta_0 = 0 \tag{2}$$

A further simplification to this equation can be considered by assuming the investigated material to be at least of the monoclinic symmetry class (13 independent material constants). This assumption is reasonable, as almost every known material has a symmetry class higher than the monoclinic case. The sixth order polynomial (eq. 2) then reduces to a third order polynomial in k_3^2 (as $\beta_1 = \beta_3 = \beta_5 = 0$) and can be solved analytically. The reduction of the equation implies that the six waves, which are present in the material, can be divided in three groups of two equal waves with one going upwards and the other going downwards. The total wave field inside the plate is then represented by a linear combination of the six different waves. In the immersion liquid (water), only two waves (up- and down going longitudinal waves) exist as a fluid does not support shear forces.

Next, assuming a parallel plate consisting of a single layer surrounded by a fluid, a model for the reflected and transmitted waves can be formulated by coupling the different wave fields inside the fluid (incident, reflected and transmitted) to the fields inside the material using the appropriate boundary conditions: continuity of the normal

displacement and normal stresses. After some tedious calculations, the complex valued reflection (eq. 3) and transmission coefficient (eq. 4) for a specific incidence angle (θ,φ) and frequency ω can be expressed as[19,20]:

$$R(\theta,\varphi,\omega) = \frac{AS - Y^2}{(S+iY)(A-iY)} \tag{3}$$

$$T(\theta,\varphi,\omega) = \frac{iY(A+S)}{(S+iY)(A-iY)} \tag{4}$$

where A and S respectively correspond to the anti-symmetric and symmetric guided wave modes propagating in the plate, while Y represents the coupling of the immersion fluid with the material plate.

The frequency spectrum of the scattered time signal of an ultrasonic pulse can now be constructed by a simple multiplication of the incident wave spectrum and the transmission or reflection coefficient. Applying the inverse Fourier transformation then yield the scattered wave signals. As a final action, the amplitude and TOF for a specific probing direction (i.e. a single data point in each UPS representation) can be obtained by evaluating the maximum amplitude and its associated time delay of the reconstructed wave signal in reflection and transmission. At this point, however, a small correction (eq. 5) needs to be introduced to the calculated TOF in transmission in order to properly compare simulations with actual experiments[10,11]:

$$\Delta t = \frac{d}{V_f}(1-\cos\theta) \tag{5}$$

where d denotes the thickness of the plate and V_f the (longitudinal) wave velocity of the bounding fluid. The correction term accounts for the different manners in which the TOF in transmission is calculated in the model compared to an actual TOF P-UPS experiment. Whereas the TOF in an experiment is determined by the time lag between the emitted and received signals, it is calculated in the model as the time needed for the wave to travel from the reference point (x_1,x_2,x_3) = (*0*,*0*,*0*) to the point (*0*,*0*,*d*). This subtle difference introduces an additional distance traveled inside the water, which translates itself in the time delay represented in equation 5.

Two-stage viscoelastic characterization procedure

The above introduced forward model can now be incorporated into an inverse model to infer information on various properties of the investigated material, e.g. the viscoelastic tensor. In previous papers, the current authors already introduced a scheme for the extraction of the elastic part of the material tensor from TOF P-UPS data by means of a least-squares function minimization using the genetic algorithm (GA) approach[10,16]. Assuming a general orthotropic material, a search space for nine independent variables is required for the elasticity tensor. The GA approach was chosen as it is able to efficiently explore this high dimensional search space within a reasonable time frame by relying on the principle of 'survival of the fittest'. In brief, the genetic algorithm starts by constructing an initial population of estimated variable sets for which the fitness function values are calculated. In the second step, all the individuals are ranked according to their fitness after which the best individuals are selected to compose the next generation of variable sets. This new generation contains direct copies of the best individuals of the previous generation, completed with descendants that are constructed from cross-over and mutation. This process is then repeated until an optimal set of parameters is found. This way, the solution not only evolves rapidly in the direction of the best individuals but it also provides the opportunity to seek a better solution which is not necessarily in the particular parameter area of the current generation. In the case of the elastic constant determination for an orthotropic material from TOF P-UPS data[10,16], the minimization function is a least-squares function measuring the deviation between the simulated and the experimental TOF landscape along multiple in-plane directions (i.e. considering several spokes in the polar plot simultaneously). Doing so, one includes important complementary information on the in-plane dependency of the nine elastic constants that are searched for, which gives us the opportunity to include an additional parameter (φ_e) representing the angle between the experimental reference frame and the actual material symmetry frame. Hence, the current approach relaxes the requirement to have a priori knowledge on the symmetry of the investigated material. In the second stage of the inversion procedure, the amplitude landscape of the P-UPS is used to determine the viscosity in a similar fashion. Amplitude UPS recordings are ideal for the determination of viscous properties as the amplitude of a scattered wave is linked to the energy dissipation, hence the damping (viscosity) of

the material. The elastic parameters found in stage one are used as input, although we allow marginal variations for better inversion results of the viscous parameters.

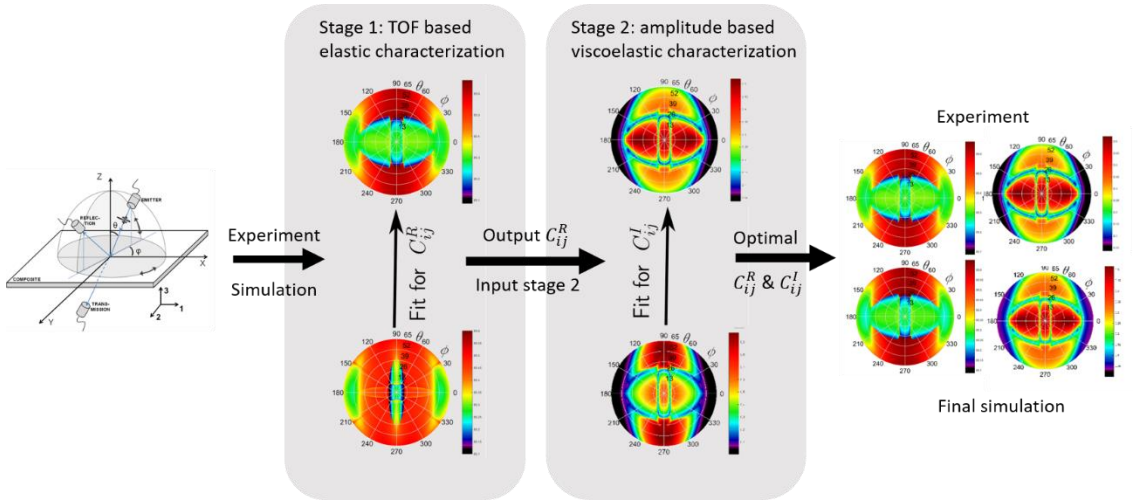

Figure 2: Graphical representation of the two-stage inversion procedure. The first stage matches the TOF landscape to infer information on the elastic constants. The second stage then fits the amplitude landscape to determine the viscous properties of the material.

RESULTS AND DISCUSION

Viscoelastic inversion procedure: synthetic data

Numerical UPS simulations in transmission (Figure 3: TOF (a) and amplitude (b)) for a viscous homogenized unidirectional C/E material of thickness 1.00 mm will be used as input for the two stage inversion approach. This will allow us to assess the performance and accuracy of the above proposed approach to retrieve the (known) input values of the viscoelastic parameters (listed in Table 1). Additionally, an angular deviation of 8° between the reference frame and the material symmetry frame has been introduced. For the simulations, an incidence angle grid $\Psi(\theta,\varphi)$ is chosen with θ going from 0° to 75° in steps of 0.1° and φ going from 0° to 360° in steps of 0.5°. The emitted time signal is modelled by a Gaussian damped cosine with a center frequency of 5 MHz and a pulse length of 10 µs. The sampling frequency is 400 Msps.

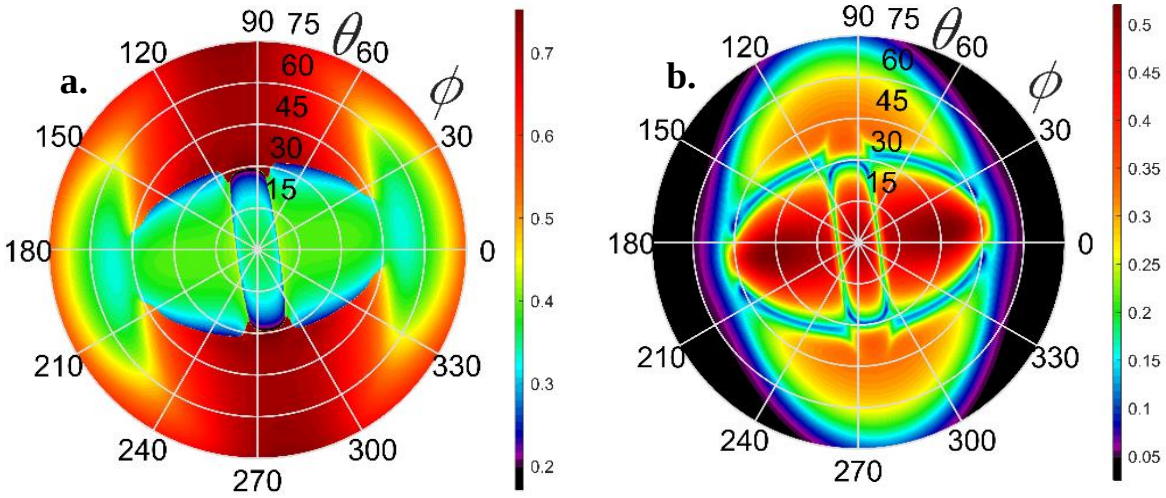

Figure 3: Synthetic TOF P-UPS (a) and amplitude P-UPS (b) images for an unidirectional C/E plate (d = 1.00 mm) with viscoelastic material parameters given in table 1. Simulations are performed with a Gaussian damped sine with central frequency of f_c = 5 MHz. The TOF colorbar in µs, the amplitude colorbar is normalized to the amplitude of the input signal.

Stage I: elastic characterization

The bounds between which the algorithm searches for the optimal elastic tensor values were set to ± 50% of the input values of the simulation. The inversion incidence angle grid takes 20 equidistant φ directions between 0° and 90° and 300 angles between 0° and 50° for the θ angles. During the first stage, a random amount of viscosity, ranging between 0.2 and 10% of the elastic constants, was introduced in the model such that the slight influence of the viscosity on the TOF values has to some extent been taken into account. The results for the first stage of the characterization process are represented in Table 1, and show that the inverted elastic properties agree well with the actual elastic parameters (error < 1.50%). In addition, the algorithm also successfully inferred the deviation angle related to the symmetry axis orientation for which it finds a value of 7.91° ± 0.59°, which is in good agreement with the input value of 8°.

TABLE 1. Elastic constants determined by way of the TOF P-UPS procedure (stage 1) for an artificial C/E material. Statistics are obtained after performing the inversion procedure 200 times.

Elastic constant	Actual C_{ij} [GPa]	Inverted C_{ij} [GPa]	Deviation [%]
C_{11}	122.73 – 8.591i	124.06±7.05	1.09
C_{12}	6.57 – 0.460i	6.54±0.44	0.39
C_{13}	6.57 – 0.460i	6.47±0.46	1.44
C_{22}	13.47 – 0.943i	13.48±0.50	0.13
C_{23}	6.55 – 0.459i	6.50±0.34	0.79
C_{33}	13.47 – 0.943i	13.67±0.53	1.50
C_{44}	3.40 – 0.238i	3.34±0.23	1.84
C_{55}	5.86 – 0.410i	5.81±0.30	0.84
C_{66}	6.25 – 0.438i	6.26±0.19	0.23

Stage II: viscoelastic characterization

In the second stage of the inversion procedure, the optimized elastic constants of the first stage are used as input. However, in contrast to what is assumed in stage 1 of the inversion, elasticity and viscosity are not entirely uncoupled in the TOF P-UPS data. Therefore, small corrections on the elasticity constants of stage one need to be allowed while determining the viscous parameters. In the present study, a small region of variability (± 5%) is admitted for the nine elasticity outputs of stage one and an inversion for both viscosity and elasticity is performed. For the viscosity parameters, the bounds are taken ± 50% of the actual viscosity parameters used in the forward numerical model.

The results of the second stage inversion for the numerical experiment are listed in Table 2 and visualized in figures 4a and 4b. The agreement between targeted and inverted values is excellent for both elasticity (<1.8%) and viscosity (<2.9%). Likewise, an excellent agreement is found between the input (8°) and inverted (7.91° ± 0.20°) reference frame misalignment. In figure 4a, a cross-section of the amplitude P-UPS simulation at φ = 60° for the inverted viscoelastic tensor is compared with the simulation based on the actual viscoelastic tensor, showing an excellent agreement. The results of the difference polar scan in figure 4b further confirms the good agreement between the inverted and the actual viscoelastic tensors as the observable deviations only occur in the regions around the characteristic contours and beyond an incident angle of θ = 50°. The deviation above θ = 50° is due to the fact that the algorithm only considers amplitude values from 0° till 50°, as beyond this θ angle certain φ directions exhibit very small amplitudes, making it difficult to accurately measure the TOF and amplitude for these incidence angles (θ,φ) in a real UPS experiment. The deviation around the contours, on the other hand, is due to the sharpness of the valleys in the amplitude landscape for transmission, which can only be recovered correctly if all input parameters of the inversion exactly match those of the numerical experiment. The presented two-stage inversion technique shows excellent results for synthetic P-UPS data. The next section investigates its capability to infer material properties from actual P-UPS experiments.

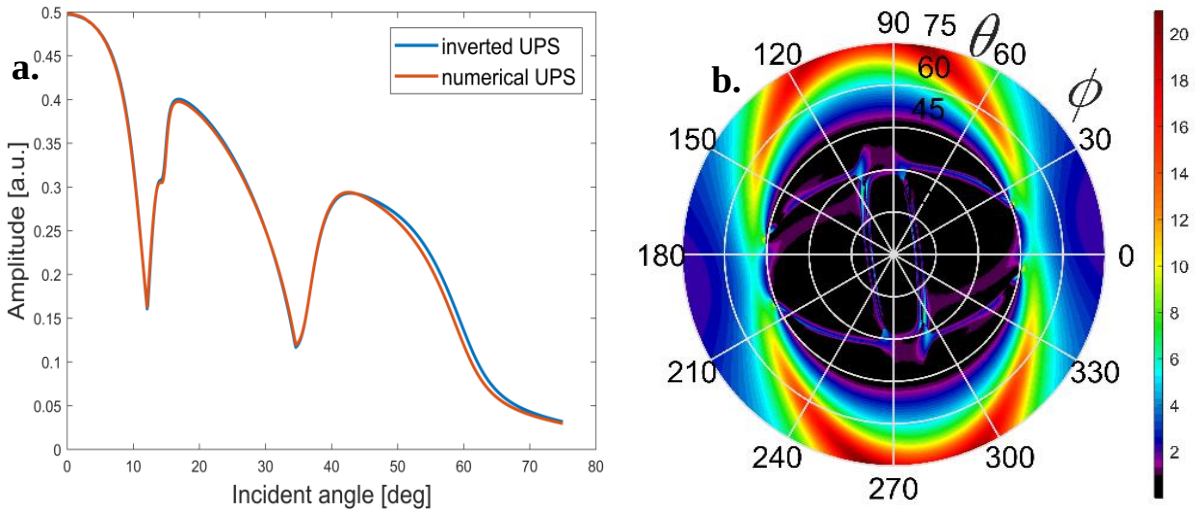

Figure 4: Cross-section of the forward amplitude P-UPS simulation at φ = 60° based on the inverted viscoelastic constants (blue) and the numerical experiment (red) (a). Difference amplitude polar scan (colorbar is in %) between simulation and numerical experiment (b), showing the largest deviations in the region of the characteristic contours and beyond a θ angle of 50°.

TABLE 2. Inversion results of the viscoelastic tensor for the synthetic experiment. The statistics were obtained after 200 characterization runs

		Elastic part of tensor		Viscous part of tensor	
Tensor constant	**Actual C_{ij} [GPa]**	**Inverted C_{ij} [GPa]**	**Deviation [%]**	**Inverted C_{ij} [GPa]**	**Deviation [%]**
C_{11}	122.73 – 8.591i	124.05±1.43	1.08	8.837±0.512	2.870
C_{12}	6.57 – 0.460i	6.55±0.09	0.29	0.457±0.033	0.637
C_{13}	6.57 – 0.460i	6.47±0.09	1.48	0.459±0.029	0.129
C_{22}	13.47 – 0.943i	13.47±0.14	0.06	0.944±0.044	0.125
C_{23}	6.55 – 0.459i	6.51±0.09	0.75	0.457±0.022	0.395
C_{33}	13.47 – 0.943i	13.62±0.16	1.16	0.955±0.025	1.362
C_{44}	3.40 – 0.238i	3.34±0.04	1.81	0.238±0.015	0.029
C_{55}	5.86 – 0.410i	5.82±0.07	0.68	0.411±0.015	0.095
C_{66}	6.25 – 0.438i	6.25±0.07	0.07	0.441±0.027	0.687

Elastic characterization of unidirectional C/E plate

In this section, a first attempt is undertaken to determine the elastic properties based on actual TOF P-UPS recordings of a $[0]_4$ C/E plate. The unidirectional composite plate has a thickness of 1.2 mm. The ultrasonic time signal, used as input for the model, corresponds to the natural impulse response of the used transducer, and strongly resembles a Gaussian damped cosine with central frequency of 4 MHz. The actual recorded TOF P-UPS data is shown in Figure 5a. The deviation angle between experimental and material symmetry frame can be estimated as -20°. In this section, the discussion is limited to the determination of the elastic properties and the deviation angle between reference frame and material symmetry frame (only the first stage of the proposed two-stage procedure is considered). Figure 5b shows the difference polar scan between the experimental TOF P-UPS and the simulated TOF P-UPS based on the final inversion results for the elastic tensor listed in Table 3. Cross-sectional sectors at φ = 72° and φ = 342° are shown in Figures 6a and 6b for experiment and simulation. These graphs illustrate that the obtained elasticity values after inversion allow for a relatively good reconstruction of the experimental TOF P-UPS recording. The most substantial deviation occur in the region of the characteristic contours as was the case for the artificial P-UPS example from previous section. An additional explanation for these deviations can be found in the fact that the model assumes plane wave propagation inside the material. Finite size transducers do not generate single plane waves but a combination of plane waves. By including the boundedness of the beam one will introduce an integrating (smoothing) effect on the measured curves, which will be most strongly pronounced in regions with sharp peaks/valleys and discontinuities coinciding with the regions of the contours. Yet, even without any further correction, the inverted

values shown in Table 3 are within expectation for the investigated material. In addition, the inversion returned a deviation angle between the experimental and materials frames of -19.35° ± 0.46°, which is close to the rough estimation of approximately -20°.

TABLE 3. Inversion results of the elastic tensor for the experimental P-UPS data. The statistics were obtained after performing 200 inversions.

Elastic constant	Inverted C_{ij} [GPa]
C_{11}	113.98±11.28
C_{12}	6.44±0.74
C_{13}	5.34±0.76
C_{22}	12.98±0.57
C_{23}	5.42±0.40
C_{33}	11.78±0.14
C_{44}	2.92±0.29
C_{55}	5.40±0.62
C_{66}	5.28±0.27

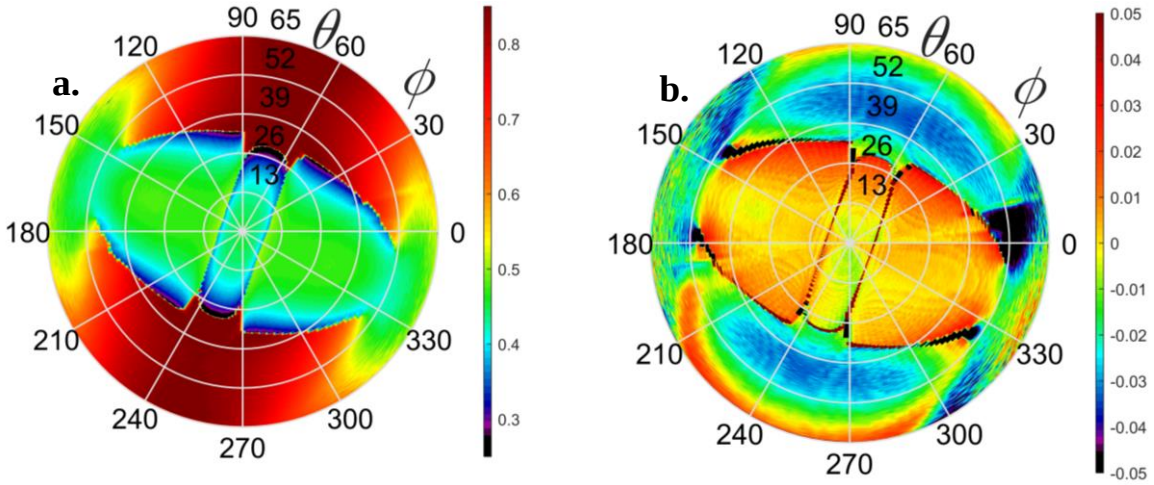

Figure 5: TOF P-UPS experiment of a [0]4 C/E plate (d = 1.2mm) insonified with the impulse response of the transducer (a). Difference polar scan image between experiment and simulated TOF P-UPS based on table 3(b). Colorbars in µs.

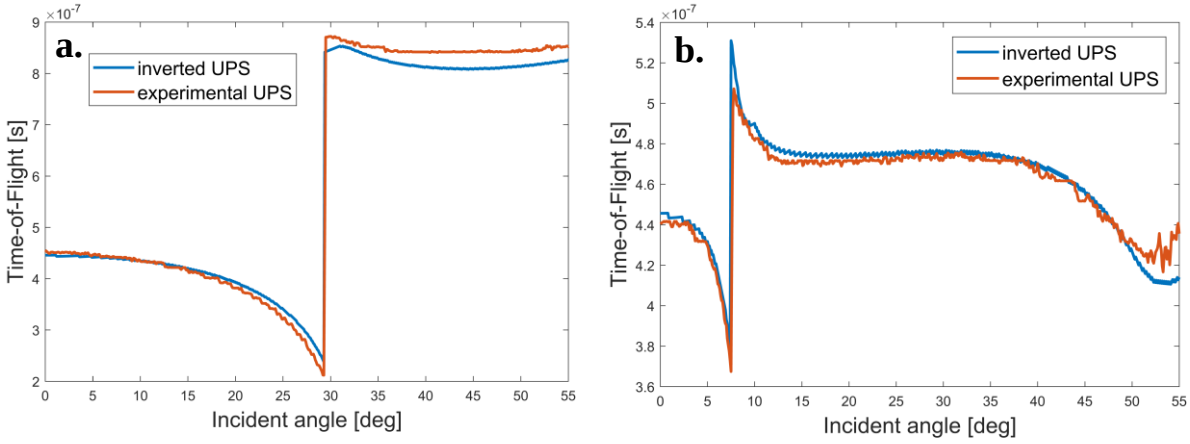

Figure 6: Cross-sectional (φ = 72°(a), φ = 342° (b)) view of the forward TOF P-UPS simulation based on the inverted elastic constants (blue) and the experimental TOF P-UPS recordings of the $[0]_4$ C/E (red).

CONCLUSION

In this paper, a two stage inversion procedure on the basis of the ultrasonic polar scan approach is introduced for determining the viscoelastic properties of composites. Stage one of the procedure uses time of flight data to characterize the elasticity parameters of the insonified material spot. The second stage subsequently uses the output of stage one (elasticity) to invert for the viscosity parameters. Excellent results for synthetic data has been obtained, which encourages us to believe that the two-stage technique should also be capable to determine the viscoelastic tensor of actual materials.

This statement was further confirmed in the application of the first stage of the inversion procedure on a real TOF P-UPS recording of a unidirectional $[0]_4$ C/E plate. The obtained values for the elasticity are in line with expected elasticity values for unidirectional carbon-epoxy plates.

Future effort will be focused on the determination of the viscous part of the stiffness tensor and on the inclusion of the bounded beam effect into the underlying model.

ACKNOWLEDGEMENTS

Support from FWO Flanders under Grant Agreements 1S45216N and G0B9515N, and from the NVIDIA corporation are gratefully acknowledged.

REFERENCES

[1] B. Hosten, J. Acoust. Soc. Am. **89**, 2745 (1991).
[2] S.I. Rokhlin and W. Wang, Acoust. Soc. Am. **91**, 3303 (1992).
[3] A. Castellano, P. Foti, A. Fraddosio, S. Marzano, and M.D. Piccioni, Compos. Part B Eng. **66**, 299 (2014).
[4] P.W.A. Stijnman, Composites **26**, 597 (1995).
[5] S.I. Rokhlin and W. Wang, J. Acoust. Soc. Am. **86**, 1876 (1989).
[6] M. Castaings, B. Hosten, and T. Kundu, NDT E Int. **33**, 377 (2000).
[7] V. Munoz, M. Perrin, M. Pastor, H. Welemane, A. Cantarel, and M. Karama, Adv. Aircr. Spacecr. Sci. **2**, 249 (2015).
[8] B. Hosten and M. Deschamps, Acta Acust. United with Acust. **59**, 193 (1986).
[9] B. Hosten, M. Deschamps, and B.R. Tittmann, J. Acoust. Soc. Am. **82**, 1763 (1987).
[10] A. Martens, M. Kersemans, J. Daemen, E. Verboven, W. Van Paepegem, J. Degrieck, S. Delrue, and K. Van Den Abeele, Compos. Struct. **180**, 29 (2017).
[11] A. Martens, M. Kersemans, J. Degrieck, W. Van Paepegem, S. Delrue, and K. Van Den Abeele, in *Emerg. Technol. Non-Destructive Test. VI , ETNDT 2016*, edited by D. Aggelis, D. Van Hemelrijck, S. Vanlanduit, A. Anastasopoulos, and T. Philippidis (CRC Press, Brussels, Belgium, 2016), pp. 141–145.
[12] L. Wang, A.I. Lavrentyev, and S.I. Rokhlin, J. Acoust. Soc. Am. **113**, 1551 (2003).
[13] W.H.M. Van Dreumel and J.L. Speijer, Mater. Eval. **39**, 922 (1981).
[14] J. Degrieck and D. Van Leeuwen, in *Emerg. Technol. Nondestruct. Test.*, edited by D. Van Hemelrijck and A. Anastassopoulos (A.A. Balkema, Rotterdam, Patras, Greece, 1996), pp. 225–236.
[15] J. Degrieck, N.F. Declercq, and O. Leroy, Insight - Non-Destructive Test. Cond. Monit. **45**, 196 (2003).
[16] M. Kersemans, A. Martens, J. Degrieck, K. Van Den Abeele, S. Delrue, L. Pyl, F. Zastavnik, H. Sol, and W. Van Paepegem, Appl. Sci. **6**, 58 (2016).
[17] M. Kersemans, W. Van Paepegem, K. Van Den Abeele, L. Pyl, F. Zastavnik, H. Sol, and J. Degrieck, Ultrasonics **54**, 1509 (2014).
[18] M. Kersemans, A. Martens, N. Lammens, K. Van Den Abeele, J. Degrieck, F. Zastavnik, L. Pyl, H. Sol, and W. Van Paepegem, Exp. Mech. **54**, 1121 (2014).
[19] A.H. Nayfeh, *Wave Propagation in Layered Anisotropic Media - with Applications to Composites* (North Holland, 1995).
[20] S. Rokhlin, D. Chimenti, and P. Nagy, *Physical Ultrasonics of Composites* (Oxford University Press, 2011).